Kinematic limit analysis of pullout capacity for plate anchors in sandy slopes

S.B. Yu[*1], R.S. Merifield[1a], A.V. Lyamin[1b] and X.D. Fu[2c]

[1]*Centre for Geotechnical and Materials Modelling, The University of Newcastle, Australia*
[2]*School of Civil Engineering, Wuhan University, Wuhan 430072, China*

Abstract.   The pullout capacity of plate anchors has been studied extensively over the past 40 years. However, very few studies have attempted to calculate the pullout capacity of anchors in sandy slopes. In this paper, three upper bound approaches are used to study the effect of a sloping ground surface and friction angle on pullout capacity and failure of plate anchors. This includes the use of; simple upper bound mechanisms; the block set mechanism approach; and finite element upper bound limit analysis. The aim of this research is to better understand the various failure mechanisms and to develop a simple methodology for estimating the pullout capacity of anchors in sandy slopes.

Keywords: anchors; sand; slope; failure surface; pullout capacity; limit analysis

1. Introduction

Plate anchors are employed as foundation systems for structures requiring uplift resistance such as transmission towers, earth-retaining walls and mooring systems for offshore floating oil and gas facilities. For anchors buried in sand, most approaches involve the use of the limit equilibrium method (Meyerhof and Adams 1968, White *et al*. 2008), or are based on formulae derived from laboratory model test (Das and Seeley 1975, Rowe and Davis 1982, Murray and Geddes 1989, Khing *et al*. 1994, Dickin and Laman 2007). The use of numerical methods for anchors in sands has been summarised by Merifield *et al*. (2006), Merifield and Sloan (2006).

Depending on the project site condition or type of structure requiring support, anchors may be installed in sloping sea bed or sand-hills in desert areas (work as a part of transmission tower foundation). Although there have been many studies undertaken to investigate the pullout capacity of anchors in sand, very limited information or guidance is available with considering the situations that anchors were installed in sandy slopes. By using the limit equilibrium method, Choudhury and Subba Rao (2007) presented seismic uplift capacity of strip anchors in $c-\varphi$ soils with inclined slope. With the exception of Kumar (1997), who proposed a simple rigid block

---

[*]Corresponding author, Ph.D., E-mail: shengbingyu@gmail.com
[a]Associate Professor, E-mail: Richard.Merifield@newcastle.edu.au
[b]Professor, E-mail: Andrei.Lyamin@newcastle.edu.au
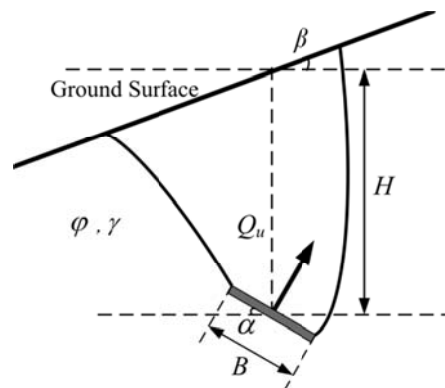[c]Professor, E-mail: xdfu@whu.edu.cn

Fig. 1 Problem notation for strip anchors in sandy slope

mechanism to produce upper bound solutions for this problem, no rigorous study has been undertaken using limit analysis method. The primary aim of this paper is to illustrate how the anchor capacity and failure mechanism changes with the angle of the ground surface, inclination angle of the anchor, and soil friction angle. A wide range of slope surface angles and anchor inclinations are considered in the current study in order to provide practical design guidelines.

2. Problem definition

A general layout of the problem to be considered is shown in Fig. 1. β is the slope angle of ground surface, B is the anchor size, Q_u is the ultimate load of anchor, φ is the friction angle of sand, and α is the inclination angle of anchor plate. The inclination angle α is positive for clockwise rotation of the anchor and negative otherwise. Then $\alpha=-\beta$, means that the anchor is parallel to the slope surface. Note that both α and β are measured form horizontal direction. But β is always positive. H is the embedment depth of anchor, which is defined as the vertical distance from the middle point of strip anchor to the ground surface. The direction of pullout is perpendicular to the anchor face. A rigid plate anchor with no thickness was assumed in the present paper.

The ultimate pullout capacity of anchors in sand can usually be expressed in the following form

$$q_u = \frac{Q_u}{A} = \gamma H N_\gamma \tag{1}$$

where A is the area of anchor, $A=B$ for the plain strain condition, γ is the unit weight of soil, and N_γ is the pullout factor for a plate anchor in sand.

3. Upper bound solution methods used

Three upper bound solution methods have been used to estimate the pullout capacity of anchors in this paper. This includes the use of simple rigid block upper bound mechanisms, the block set mechanism approach (Yu 2011), and finite element upper bound limit analysis.
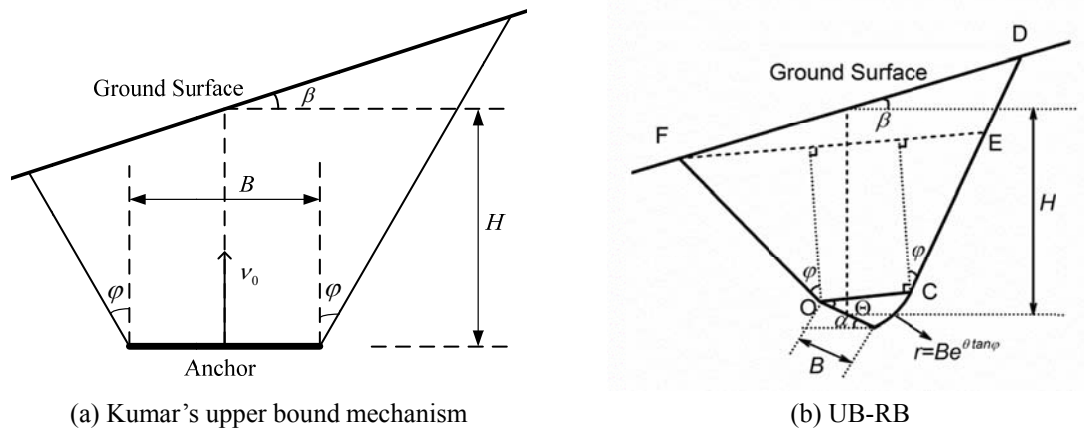
(a) Kumar's upper bound mechanism   (b) UB-RB

Fig. 2 Simple upper bound rigid block mechanism for anchors in sandy slopes

3.1 Simple rigid block upper bounds (UB-RB)

Kumar (1997) proposed a simple mechanism, which is shown in Fig. 2(a), to produce upper bound solutions of pullout capacity of plate anchors buried in sandy slope. Kumar (1997) indicated that the pullout capacity of horizontal anchors, even in sloping ground, remains the same as that for a horizontal ground surface for equal embedment ratios (H/B).

A better representation of the collapse mechanism, and therefore a more accurate estimate of the pullout capacity for anchors in sloping ground, can be obtained from newly developed mechanism proposed in this paper (Fig. 2(b)). In brief the new mechanism consists of a logspiral shear zone and a quadrilateral rigid block, with more details given in Appendix A along with the derivation of the pullout factor N_γ. The results from the upper bound mechanisms shown in Fig. 2(b) will be compared with the remaining solution methods discussed below.

3.2 Upper bound block set mechanism (UB-BSM)

The pullout capacity can also be obtained using the block set mechanism (Yu 2011), which is based on multi-rigid blocks and can give an explicit failure surface. For block set mechanism, a type of combination of basic block set is used to construct more complicated admissible velocity field. As shown in Fig. 3(a), Part ① and Part ② are the basic block sets, while Part ③ and Part ④ are the triangular blocks. The basic block sets with a polar coordinate system is also shown in Fig. 3(a), where the point O is the pole and ρ_i is the radius. The basic block set consists of N triangular rigid wedges, and described by N angular parameters $\left[\delta\theta_i \left(i = 1, ..., N \right) \right]$ and $N+1$ radius parameters $\left[\rho_i \left(i = 1, ..., N+1 \right) \right]$. θ_1 and θ_2 are the start angle and end angle of basic block set. Thus, the swept area of basic block set is confined to the range θ_1 to $2\pi - \theta_2$. If taking $\left[\rho_i \left(i = 1, ..., N+1 \right) \right]$, θ_1 and θ_2 as variables, then various shapes of basic block set can be obtained. More details about basic block set are given in Appendix B along with the calculations of internal energy dissipation and total external work.

The admissible velocity field for strip anchor in sandy slope is constructed as shown in Fig. 3(b), in which two combination sets were used to define the shape of the failure surface. The

(a) combination set   (b) mechanism for strip anchor
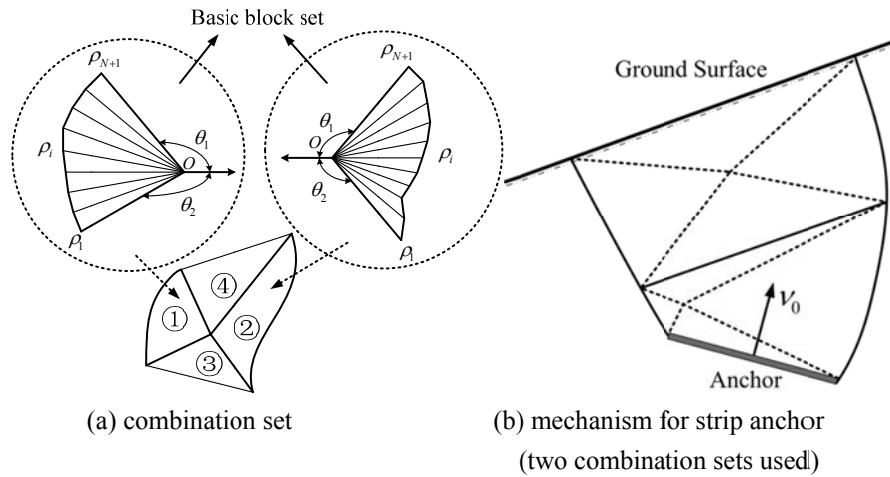
(two combination sets used)

Fig. 3 Construction schematic of admissible velocity field for anchor in sandy slope using UB-BSM

dashed lines in Fig. 3(b) show the shapes of the basic block set in each combination set. The total internal energy E is given by the sum of each internal energy of two combination sets. The total work done by the weight of soil W can also be obtained by the sum of the work done by the soil weight in the two combination sets. The work done by the pullout force Q_u is

$$F = Q_u v_0 \qquad (2)$$

where v_0 is the velocity of the strip anchor.

According to the upper bound theorem (Chen 1975), the following inequality must be satisfied:

$$F + W \leq E \qquad (3)$$

Substituting Eq. (3) and Eq. (2) to Eq. (1), the pullout factor of anchor in sand can be expressed as

$$N_\gamma \leq \frac{E - W}{B v_0 \gamma H} \qquad (4)$$

A hybrid genetic algorithm (GA) combined with pattern search method (or named direct search method) is used to find the minimum value of pullout factor N_γ from Eq. (4). To illustrate the use of two combination sets, the failure surfaces of a horizontal anchor in horizontal ground and sloping ground after optimization are shown in Fig. 4(a) and (b) respectively, in which the detail of each combination set is also shown. Since the final mechanism may contain hundreds of triangular rigid wedges, the triangular rigid wedges of each basic block set are denoted concisely by the different symbols (little triangle and circles). From the comparison of the failure surfaces shown in Fig. 4(a) and Fig. 4(b), it can be seen that the sloping ground has a great influence on the shapes of the combination set. For anchors in sandy slopes, the 2nd combination set was degenerated to one basic block set in the final results, which is shown in Fig. 4(b). For an anchor as shown in Fig. 4(a), the borderline between the 1st and 2nd combination set is a horizontal line, and there is no relative movement between two combination sets in the final results.
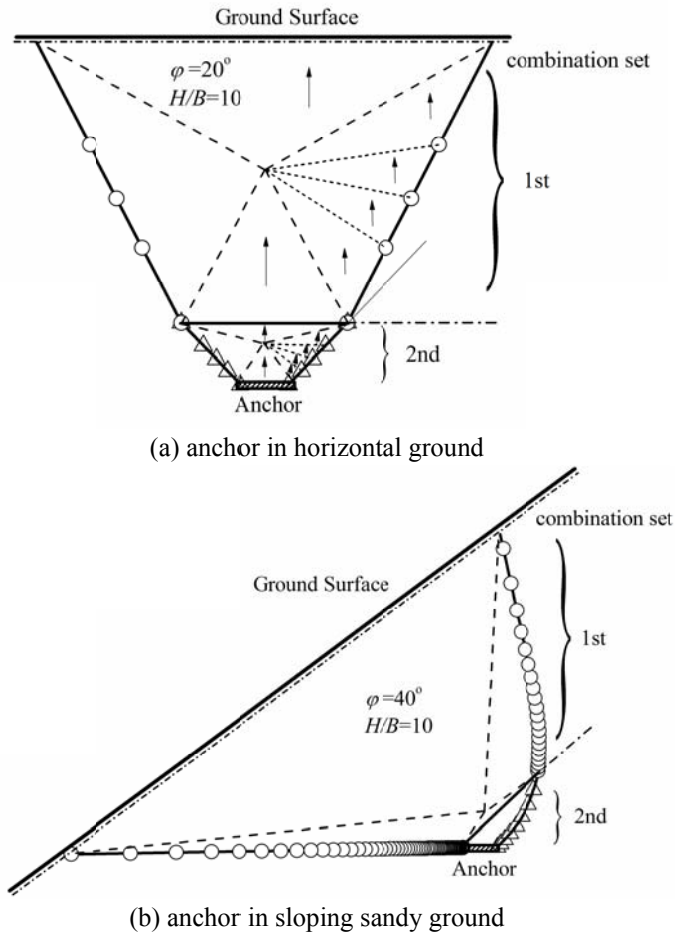
(a) anchor in horizontal ground

(b) anchor in sloping sandy ground

Fig. 4 UB-BSM failure surface of anchor in horizontal and sloping sandy ground after optimization

3.3 Upper bound finite element limit analysis (UB-FELA)

Rigorous bounds on the ultimate pullout load presented in this paper are also obtained by using the finite element (FE) upper bound (UB) and lower bound (LB) formulations developed by Lyamin and Sloan (2002a, b), and Krabbenhoft *et al*. (2005) that are based on finite element formulations of the upper and lower bound theorems of limit analysis. These formulations assume a perfectly plastic soil model with an associated flow rule and have been used successfully to model anchors in clay and sand previously by Merifield *et al*. (2001, 2005, 2006). Readers are referred to these original papers published on the UB and LB formulations for further details.

4. Results and discussion

Upper bound analyses using the methods outlined above were performed to obtain estimates of the pullout factor N_γ and failure surface of anchors in sandy slopes, for the range of embedment

ratios (H/B) from 1 to 10, slope angle β from 0° to 40° and anchor inclination angles of α from -30° to 90°. These results are discussed in the following sections. Where possible, past experimental and numerical results are compared with results obtained from the current study.

4.1 Inclined anchors in horizontal ground

For the ranges of incline angle α from 0° to 90°, comparisons of pullout capacity factors of inclined anchors in horizontal ground are shown in Fig. 5(a)-(c). For horizontal anchors, comparisons of pullout capacities from the current study against existing upper bound solutions are shown in Fig. 5(a). For horizontal anchors in horizontal ground, the simple mechanism proposed in this paper (where β=0 and Θ=0) is the same as the simple mechanism shown in Fig. 2(a) (when β=0). It can be seen that the solutions of the block set mechanism and simple mechanism are very close to each other, and are lower than that of the finite element limit analysis (Merifield and Sloan 2006). Although there is a difference between failure surfaces considered in the simple mechanism and block set mechanism, the value of pullout capacities seems to be not very sensitive to these failure surface differences.
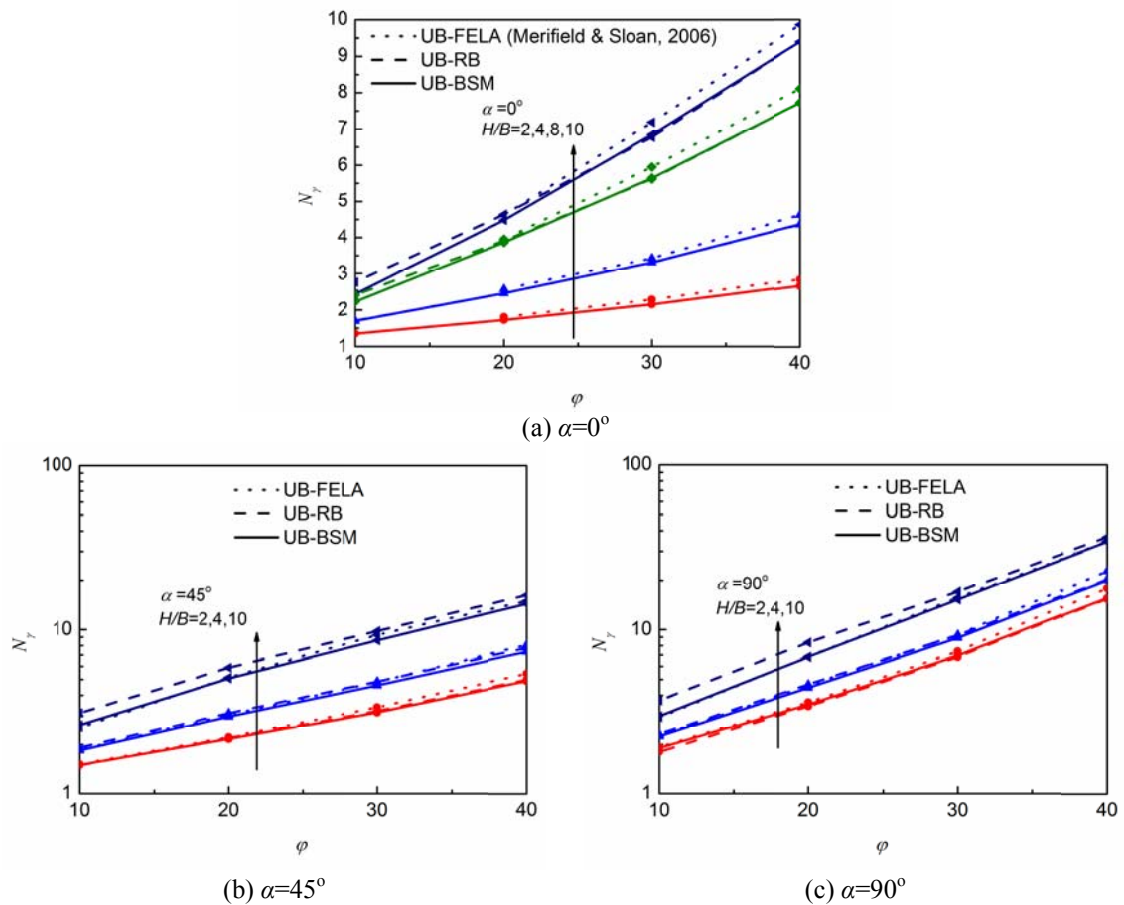

(a) α=0°

(b) α=45°

(c) α=90°

Fig. 5 Pullout capacity of inclined anchors in horizontal ground

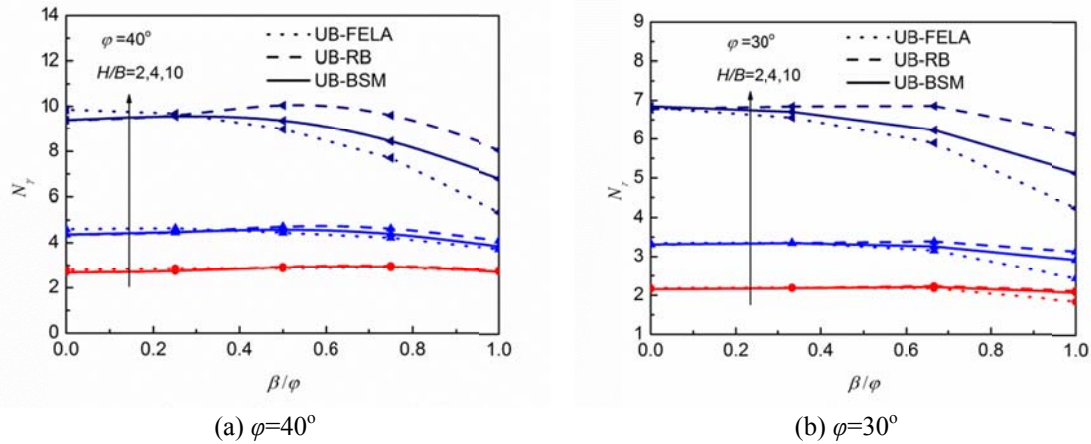(a) $\varphi=40^{\circ}$ (b) $\varphi=30^{\circ}$

Fig. 6 Pullout capacity of horizontal anchors in sandy slopes

For inclined anchors, the active failure may develop behind the anchor and there will be soil falling in this zone. For upper bound limit analysis, this means that if one takes this active failure into consideration, a smaller upper bound collapse load will be predicted (Merifield 2002). However, both the simple mechanism and block set mechanism adopted in this paper did not take this into account. As shown in Fig. 5, the pullout capacity of the anchor increases with increasing inclination angle of the anchor and internal friction angle of sand. It can be seen that there is a reasonable agreement among the solutions from all three approaches employed. For larger anchor embedment ratio H/B shown in Fig. 5(b) and (c), the finite element method predicts the lowest upper bound solution. However, the other two upper bound solutions are not very far apart. Although the UB-FELA approach is much more complex than the other two upper bound approaches, it indicated that the UB-RB and UB-BSM can also give a very good solution for the anchors in horizontal ground. Hence, the UB-RB approach will be a better choice for this case as it is easy-to-use and with enough accuracy of solution.

4.2 Horizontal anchors in sandy slopes

Since the soil is considered as cohesionless, the slope angle β must be less than the friction angle φ of sand ($\beta<\varphi$) so that the slope itself remains always stable. Note that, in the case when the slope angle β is close to the friction angle φ, the problem will become the stability problem of slope induced by pullout of anchor, and the pullout capacity of anchors in such situation is immaterial in practical design. Therefore, these cases are out of focus of this paper and will not be discussed herein.

For the range of β/φ from 0 to 1 and for $\varphi=30^{\circ}$ and 40° comparisons of pullout capacity factors of anchors in sandy slopes are shown in Fig. 6. It is clearly seen that there is a trend of reduction in the pullout capacity of anchors in slopes with increasing the slope angle and anchor embedment ratio. In the extreme case, when H/B=10, $\varphi=40^{\circ}$ and $\beta=30^{\circ}$, the reduction in pullout capacity will be more than 20%. However, for anchors at small embedment ratios, the reduction of pullout capacity is less significant. It can be seen that, for anchors at small embedment ratios, the three upper bound solutions are very close to each other. But for anchors at larger embedment ratios and

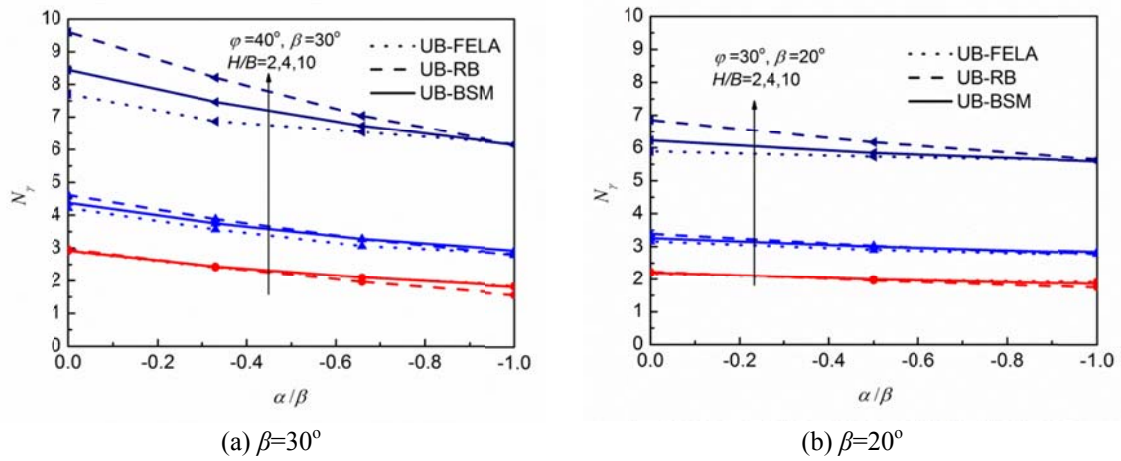(a) *β*=30°   (b) *β*=20°

Fig. 7 Pullout capacity of inclined anchors in sandy slopes

greater slope angles, the discrepancy among these three solutions becomes apparent. In current study, generally 4000-6000 elements were used for UB-FELA, tens or hundreds of rigid blocks for UB-BSM, and a logspiral shear zone with a quadrilateral rigid block for UB-RB. From this comparison, it is obvious that the UB-FELA uses much more variables to describe the velocity field, so it has more capability to deal with the complex problems. As shown in Fig. 6, UB-FELA gives significantly smaller upper bound solution for anchors for greater slope angles and anchor embedment ratios comparing to other methods. But for the other cases, this advantage is not so obvious. It means that for these cases the velocity field is much more simple and it is unnecessary to use so many variables to describe it.

4.3 Inclined anchors in sandy slopes

For inclined anchors in sandy slopes with inclination angle $\alpha > 0$, the pullout capacity will be larger comparing to similar anchors in horizontal ground. Therefore, for practical purposes, only cases with $\alpha < 0$ will be analyzed in this section.

Comparisons of pullout capacity factors of inclined anchors in sandy slopes are shown in Fig. 7. It can be seen that the pullout capacity decreases with the increase in inclination angle of the anchor. Also, with increasing the inclination angle of the anchor, the discrepancy between all upper bound methods employed becomes smaller. For the case when the anchor is parallel to the slope surface ($\alpha = -\beta$), the three upper bound solutions are almost the same.

In Fig. 8 the plastic zones and failure surfaces for UB-FELA and UB-BSM, respectively, are compared (the black solid line being the failure surface obtained from UB-BSM). Looking at Figs. 8(a) and (b), it can be concluded that the discrepancy between failure surface and plastic zones is mainly observed on the downside part of the slope. Since UB-FELA takes into account the slope failure induced by pullout of anchor, the extent of plastic zones on the downside of the slope is much larger than one predicted by UB-BSM. It is worth to emphasize here that only pullout of anchor from the ground is considered when constructing of UB-BSM mechanism. For anchors in horizontal ground(shown in Figs. 8(c) and (d)), the failure surface and plastic zones are in reasonable agreement.
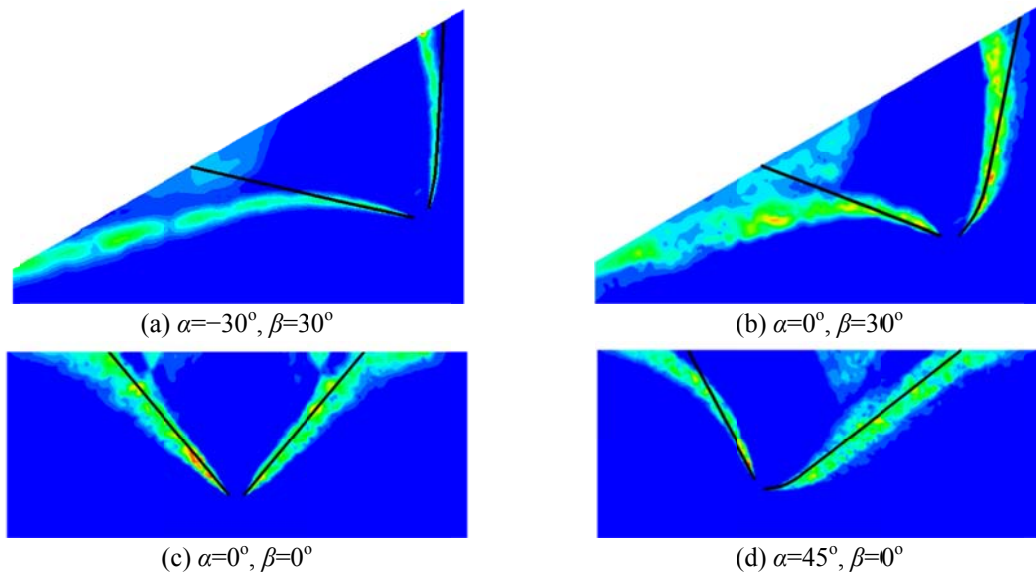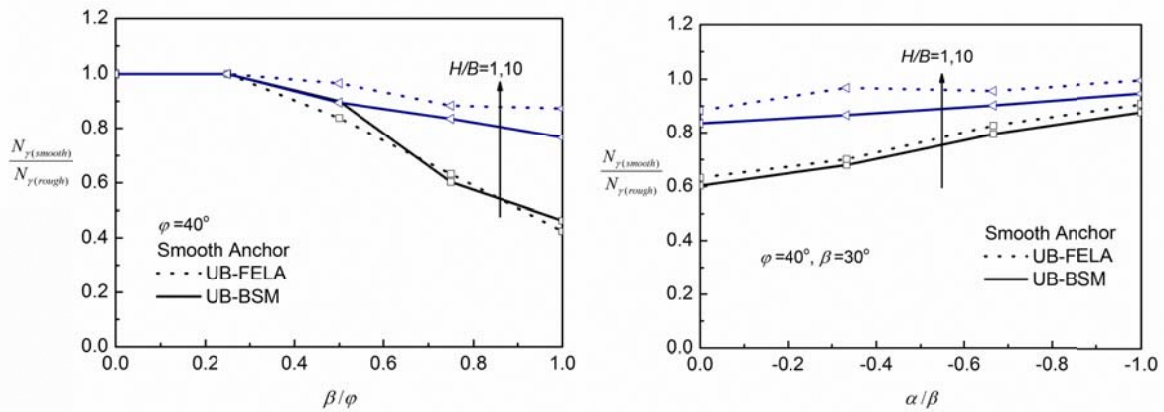
(a) $\alpha=-30^{\circ}$, $\beta=30^{\circ}$

(b) $\alpha=0^{\circ}$, $\beta=30^{\circ}$

(c) $\alpha=0^{\circ}$, $\beta=0^{\circ}$

(d) $\alpha=45^{\circ}$, $\beta=0^{\circ}$

Fig. 8 Comparison of plastic zones (UB-FELA) and failure surface (UB-BSM) (H/B=10, $\varphi=40^{\circ}$)

(a) horizontal anchor in different sandy slope　　(b) different anchor inclination in sandy slope

Fig. 9 Effect of roughness

It can be also noticed that as the anchor tends to be parallel with the slope surface, the failure surface becomes a straight line. It means that fewer variables can be used to obtain an accurate solution. Hence, although the UB-RB technique is much simpler than the UB-FELA, it gives a better solution for larger inclination angle of strip anchor and smaller embedment ratios.

4.4 Effect of anchor roughness

For a horizontal anchor in horizontal ground, only one triangular rigid block is in contact with the anchor plate for UB-BSM as shown in Figs. 3 and 4. Due to this fact, there are not enough degrees of freedom to reflect the influence of the anchor roughness. As result, the numerical results

(a) inclined anchor in sandy slope   (b) vertical anchor in sand
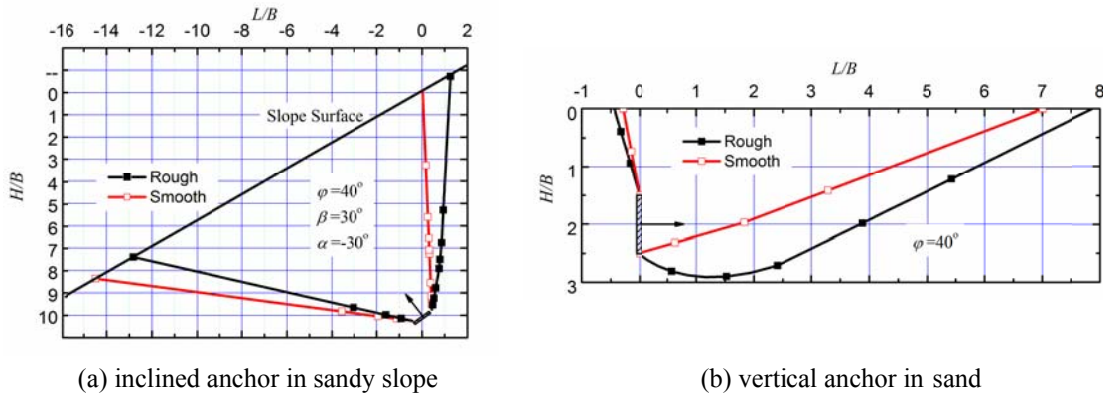
Fig. 10 Comparison of failure surface for smooth and rough anchors in sandy

are unchanged for the UB-BSM in this case, regardless of the anchor roughness. On the other hand, as shown in Fig. 9(a) where UB-FELA results are presented, the effect of anchor roughness for this problem set up is minor. This agrees with the findings of Merifield and Sloan (2006).

Fig. 9 compares the upper bound solutions obtained by UB-BSM and UB-FELA for anchors in sandy slopes. It shows that the pullout capacity of smooth anchors is smaller than that of rough anchors. For smooth anchors at greater slope angles, there is a more pronounced reduction in pullout capacity. Generally, the solutions of smooth anchor from UB-BSM and UB-FELA are close to each other. This can be verified by the comparing the failure surfaces of smooth and rough anchors. As shown in Fig. 10, it can be seen that the former one tends to be a straight line, while the later one is curved. Therefore, the discrepancy between UB-BSM and UB-FELA solutions for smooth anchor is not so obvious as that for the rough anchor case.

5. Conclusions

Upper bound analyses for pullout capacity together with failure surfaces of strip anchors in sandy slopes have been presented. Consideration has been given to the effects of sloping ground surface and friction angle on pullout capacity and failure of plate anchors. It was found that there is a reduction in pullout capacity for anchors in sandy slopes comparing to horizontal surface. And this reduction increases with increasing the slope angle and inclination of anchor. Through comparison among three different upper bound approaches, it indicated that, for the case that anchors are parallel with the slope ground or anchors in horizontal ground, there is no significant difference on upper bound pullout capacities of anchors. For practical application, UB-RB approach will be a better choice for this case as it is easy-to-use and with enough accuracy of solution. For other cases that anchors are in sandy slope, UB-FELA and UB-BSM would be recommended for practical design since UB-RB approach will heavily overestimate the pullout capacity of anchors. Overall, the primary focus of this paper is to develop a simple methodology for estimating the pullout capacity of anchors in sandy slopes by employing various methods of analysis.

References

Chen, W.F. (1975), *Limit analysis and soil plasticity*, Elsevier Science & Technology.

Choudhury, D. and Subba Rao, K.S. (2007), "Generalized solution for seismic uplift capacity of strip anchors using pseudo-static approach", *J. Earthq. Tsunami*, **1**(4), 311-328.

Das, B.M. and Seeley, G.R. (1975), "Breakout Resistance of Shallow Horizontal Anchors", *J. Geotech. Eng. Div.*, **101**(9), 999-1003.

Dickin, E.A. and Laman, M. (2007), "Uplift response of strip anchors in cohesionless soil", *Adv. Eng. Softw.*, **38**(8-9), 618-625.

Khing, K.H., Das, B.M. and Yen, S.C. (1994), *Uplift capacity of strip plate anchors in clay with sloping surface*, International Society of Offshore and Polar Engineers, Osaka,Japan.

Krabbenhoft, K., Lyamin, A.V., Hjiaj, M. and Sloan, S.W. (2005), "A new discontinuous upper bound limit analysis formulation", *Int. J. Numer. Meth. Eng.*, **63**(7), 1069-1088.

Kumar, J. (1997), "Upper bound solution for pullout capacity of anchors on sandy slopes", *Int. J. Numer. Anal. Meth. Geomech.*, **21**(7), 477-484.

Lyamin, A.V. and Sloan, S.W. (2002a), "Lower bound limit analysis using non-linear programming", *Int. J. Numer. Method. Eng.*, **55**(5), 573-611.

Lyamin, A.V. and Sloan, S.W. (2002b), "Upper bound limit analysis using linear finite elements and non-linear programming", *Int. J. Numer. Anal. Meth. Geomech.*, **26**(2), 181-216.

Merifield, R.S. (2002), Numerical modelling of soil anchors, University of Newcastle, Australia

Merifield, R.S., Lyamin, A.V. and Sloan, S.W. (2005), "Stability of inclined strip anchors in purely cohesive soil", *J. Geotech. Geoenviron. Eng.*, **131**(6), 792-799.

Merifield, R.S., Lyamin, A.V. and Sloan, S.W. (2006), "Three-dimensional lower-bound solutions for the stability of plate anchors in sand", *Geotechnique*, **56**(2), 123-132.

Merifield, R.S. and Sloan, S.W. (2006), "The ultimate pullout capacity of anchors in frictional soils", *Can. Geotech. J.*, **43**(8), 852-868.

Merifield, R.S., Sloan, S.W. and Yu, H.S. (2001), "Stability of plate anchors in undrained clay", *Geotechnique*, **51**(2), 141-153.

Meyerhof, G.G. and Adams, J.I. (1968), "The ultimate uplift capacity of foundations", *Can. Geotech. J.*, **5**(4), 225-244.

Murray, E.J. and Geddes, J.D. (1989), "Resistance of passive inclined anchors in cohesionless medium", *Geotechnique*, **39**(3), 417-431.

Rowe, R.K. and Davis, E.H. (1982), "The behaviour of anchor plates in sand", *Geotechnique*, **32**(1), 25-41.

White, D.J., Cheuk, C.Y. and Bolton, M.D. (2008), "The uplift resistance of pipes and plate anchors buried in sand", *Geotechnique*, **58**(10), 771-779.

Yu, S.B. (2011), "Block set mechanism for upper bound analysis and its applications", Ph.D Thesis, Tongji University, Shanghai

Appendix A

As shown in Fig. 2(b), the pullout capacity of anchor can be divided into three parts, which are come from logspiral shear zone, isosceles trapezoid OCEF and triangle FED.

For the logspiral shear zone, the total work done by the weight of soil W_1 is

$$W_1 = -\frac{1}{2}\gamma B^2 v_0 \left\{ e^{3\Theta\tan\varphi} \frac{\sin(\Theta-\alpha)+3\tan\varphi\cos(\Theta-\alpha)}{1+9\tan^2\varphi} - e^{3(-\alpha)\tan\varphi} \frac{\sin(-\alpha)+3\tan\varphi\cos(-\alpha)}{1+9\tan^2\varphi} \right\}$$

(A1)

Substituting Eq. (A1) to Eq. (4), the pullout factor of this part can be expressed as

$$N_{1\gamma} = \frac{B}{2H} \left\{ e^{3\Theta\tan\varphi} \frac{\sin(\Theta-\alpha)+3\tan\varphi\cos(\Theta-\alpha)}{1+9\tan^2\varphi} - e^{3(-\alpha)\tan\varphi} \frac{\sin(-\alpha)+3\tan\varphi\cos(-\alpha)}{1+9\tan^2\varphi} \right\}$$

(A2)

For the isosceles trapezoid OCEF
H' is the vertical distance from the point O to the ground surface.

$$H' = H - \frac{1}{2}B\cos\alpha\tan\beta - \frac{1}{2}B\sin\alpha$$

(A3)

$$OF^2 = H'^2 \frac{1+\cot^2(\Theta-\alpha+\varphi)}{(\cot(\Theta-\alpha+\varphi)+\tan\beta)^2}$$

(A4)

The total work done by the weight of soil W_2 is

$$W_2 = -\left(Be^{\Theta\tan\varphi}OF\cos\varphi + OF^2\sin\varphi\cos\varphi \right)\gamma\cos(\Theta-\alpha)v_0 e^{\Theta\tan\varphi}$$

(A5)

$$N_{2\gamma} == \frac{e^{2\Theta\tan\varphi}OF\cos\varphi\cos(\Theta-\alpha)}{H} + \frac{OF^2\sin\varphi\cos\varphi\cos(\Theta-\alpha)e^{\Theta\tan\varphi}}{BH}$$

(A6)

For the triangle FED

$$EF^2 = B^2 e^{2\Theta\tan\varphi} + 4OF^2\sin^2\varphi + 4Be^{\Theta\tan\varphi}OF\sin\varphi$$

(A7)

The area of triangle FED is

$$S_{\Delta EFD} = \frac{1}{2}\left(B^2 e^{2\Theta\tan\varphi} + 4OF^2\sin^2\varphi + 4Be^{\Theta\tan\varphi}OF\sin\varphi \right)\frac{\cos\varphi\sin(\beta-\Theta+\alpha)}{\cos(\Theta-\alpha-\varphi-\beta)}$$

(A8)

The total work done by the weight of soil W_3 is

$$W_3 = -S_{\Delta EFD}\gamma\cos(\Theta-\alpha)v_0 e^{\Theta\tan\varphi}$$

(A9)

$$N_{3\gamma} = \left(\frac{B\,e^{3\Theta\tan\varphi}}{2H} + \frac{2OF^2\sin^2\varphi}{BH}e^{\Theta\tan\varphi} + \frac{2e^{2\Theta\tan\varphi}OF\sin\varphi}{H} \right) \frac{\cos(\Theta-\alpha)}{\cot(\beta-\Theta+\alpha)-\tan\varphi} \quad \text{(A10)}$$

The pullout factor of anchor can be obtained by the sum of pullout factor from three parts.

$$N_\gamma = N_{1\gamma} + N_{2\gamma} + N_{3\gamma} \quad \text{(A11)}$$

This simple mechanism contains a variable Θ, so lower upper bound must be obtained by optimization.

Appendix B

The basic block sets with a polar coordinate system in the clockwise or counterclockwise direction shown in Fig. B1 are considered, where the point O is the pole and ρ_i is the radius. The basic block set consists of N triangular rigid wedges, and described by N angular parameters $[\delta\theta_i(i=1,\ldots,N)]$ and $N+1$ radius parameters $[\rho_i(i=1,\ldots,N+1)]$. To facilitate presentation, the triangular rigid wedges are numbered as ①, ②, ③, ④…; and θ_1 and θ_2 are the start angle and end angle of basic block set. Thus, the swept area of basic block set is confined to the range θ_1 to $2\pi-\theta_2$. Now consider the case in the clockwise direction which is shown in Fig. B1(b). In this case, the parameters of triangular rigid wedge numbered i are given in Fig. B2, where α_i, β_i and $\delta\theta_i$ are the three angles of triangular wedge i; d_i, ρ_i and ρ_{i+1} are the three sides respectively; ξ_{i+1} is the angle between d_i and d_{i+1}; v_i is the velocity of triangular rigid wedge i; and $v_{r(i+1)}$ is the relative velocity of triangular wedge $i+1$ with respect to triangular wedge i. According to the normality rule, the velocity jump on every discontinuity surface should be inclined at an angle φ with the surface, where φ is the friction angle of soil in which the discontinuity surface lays.

Geometrical characteristics of the triangular wedge i are presented in the following equations

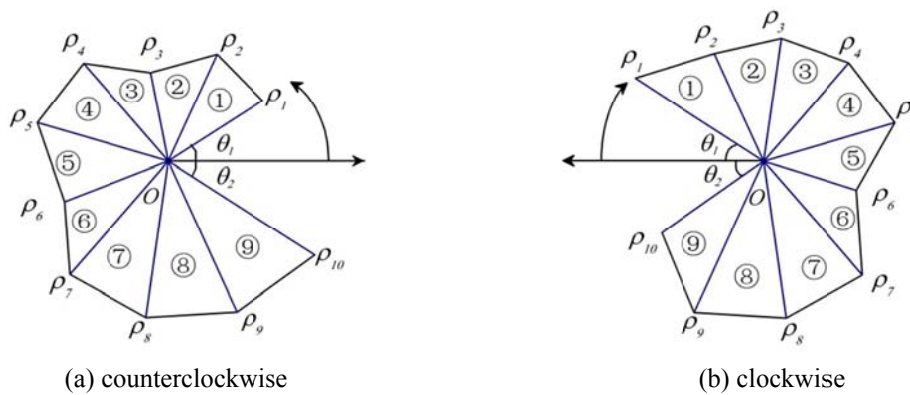$$d_i = \sqrt{\rho_i^2 + \rho_{i+1}^2 - 2\rho_i\rho_{i+1}\cos\delta\theta_i} \quad \text{(B1)}$$

(a) counterclockwise   (b) clockwise

Fig. B1 Schematic view for basic block sets
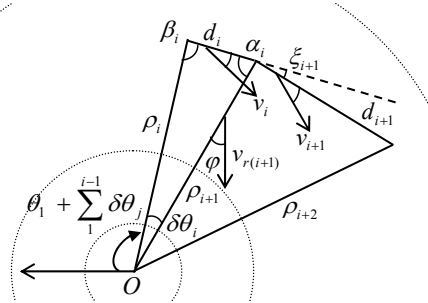
Fig. B2 Parameters of triangular wedge i

(a) $\xi_{i+1} \geq 0$ (b) $\xi_{i+1} < 0$
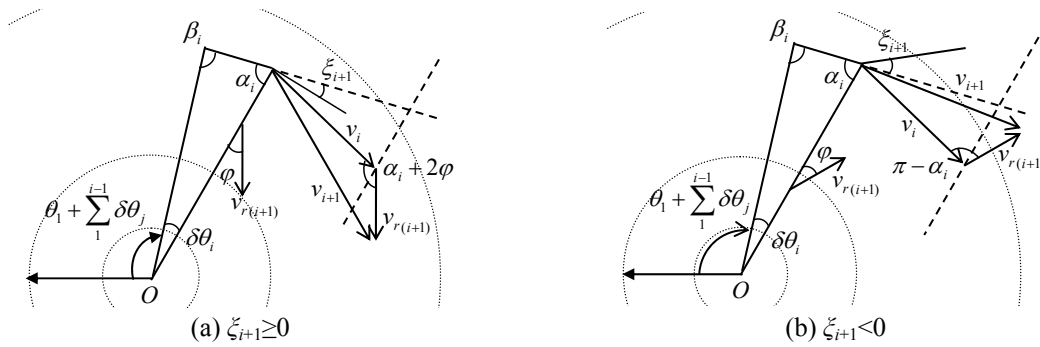
Fig. B3 Velocity hodograph of basic block set

$$\alpha_i = \arccos\left(\frac{d_i^2 + \rho_{i+1}^2 - \rho_i^2}{2 d_i \rho_{i+1}}\right) \tag{B2}$$

$$\beta_i = \pi - \alpha_i - \delta\theta_i \tag{B3}$$

$$\xi_i = \pi - \alpha_{i-1} - \beta_i \tag{B4}$$

$$\zeta_{i+1} = \zeta_i + \xi_{i+1} \tag{B5}$$

where ζ_i is the azimuth of velocity v_i in the polar coordinate system, and $\zeta_1 = \theta_1 + \pi - \beta_1 + \varphi$.

As shown in Fig. B3, the velocity hodograph for two adjacent rigid wedges can be divided into two cases. The velocity of each triangular rigid wedge in basic block set can be determined in a certain order.

Case 1: $\xi_{i+1} \geq 0$

From the velocity hodograph of Fig. B3(a), the angle between v_i and v_{i+1} is ξ_{i+1}; and the angle between v_i and $v_{r(i+1)}$ is $\alpha_i + 2\varphi$. Thus, the velocities v_{i+1} and $v_{r(i+1)}$ can be calculated from the velocity v_i as follows

$$v_{i+1} = \frac{\sin(2\varphi + \alpha_i)}{\sin(\beta_{i+1} - 2\varphi)} v_i \tag{B6}$$

$$v_{r(i+1)} = \frac{\sin(\alpha_i + \beta_{i+1})}{\sin(\beta_{i+1} - 2\varphi)} v_i \tag{B7}$$

where i takes values from 1 to N-1 and N is the total number of triangular rigid wedges used in the basic block set.

Case 2: $\xi_{i+1} < 0$

From the velocity hodograph of Fig. B3(b), the angle between v_i and v_{i+1} is $-\xi_{i+1}$; the angle between v_i and $v_{r(i+1)}$ is $\pi - \alpha_i$. Thus, the velocities v_{i+1} and $v_{r(i+1)}$ are

$$v_{i+1} = \frac{\sin \alpha_i}{\sin \beta_{i+1}} v_i \tag{B8}$$

$$v_{r(i+1)} = -\frac{\sin(\alpha_i + \beta_{i+1})}{\sin(\beta_{i+1})} v_i \tag{B9}$$

For the basic block set, the total internal energy dissipated on the velocity discontinuities is given by the sum of the product of cohesion of soil c, relative velocity, length of each discontinuity and $\cos\varphi$, i.e.

$$E = \sum_1^N c d_i v_i \cos\varphi + \sum_2^N c \rho_i v_{r(i)} \cos\varphi \tag{B10}$$

and the total work done by the weight of soil is

$$W = -\sum_1^N \gamma \frac{1}{2} \rho_i \rho_{i+1} \sin(\delta\theta_i) v_i \sin\zeta_i \tag{B11}$$

where c and φ is the cohesion and internal friction angle of soil; and γ is the unit weight of soil.

Since the directions of gravity for both the clockwise and counterclockwise cases are the same as $3\pi/2$, Eqs. (B10) and (B11) are also applicable in the case of counterclockwise polar coordinate system.